RSC Advances

COMMUNICATION

View Article Online
View Journal | View Issue

Synthesis of a benzothiazole nanoporous polymer for selective CO_2 adsorption†

Cite this: *RSC Adv.*, 2014, **4**, 9669

Received 12th December 2013
Accepted 27th January 2014

DOI: 10.1039/c3ra47587e

www.rsc.org/advances

Venkata S. Pavan K. Neti,[a] Xiaofei Wu,[b] Ping Peng,[a] Shuguang Deng[b] and Luis Echegoyen*[a]

A new benzothiazole linked nanoporous polymer, imine benzothiazole polymer (IBTP), was synthesized *via* a Schiff base condensation reaction. IBTP showed high isosteric heat of adsorption (Q_{st}) (37.8 kJ mol^{-1} at 273 K) and reasonable CO_2 adsorption (7.8 wt% at 273 K/1 bar) as well as good selectivities, CO_2/N_2 (51) and CO_2/CH_4 (6.3). The Brunauer–Emmett–Teller (BET) surface area of IBTP was 328 m^2 g^{-1} and it also showed good thermal stability up to 450 °C under a N_2 atmosphere, thus showing good potential for CO_2 capture.

To date, robust porous organic polymers (POPs) have been limited to well-known imine, imide, benzimidazole and triazine organic units.[1] Other types of linkages in covalent organic frameworks (COFs), polymers of intrinsic microporosity (PIMs) and conjugated microporous polymers (CMPs) have also been explored as extended crystalline and amorphous frameworks.[1,2] Here, we describe the first example of linking benzobisthiazole functional groups within a single framework that is a highly conjugated polymer containing imine functional groups. Carbon dioxide capture using nitrogen rich imine linked COFs, metal organic frameworks[3] (MOFs), zeolitic imidazolate frameworks[4] (ZIFs) and POPs have been explored for environmental applications. These imine-linked COFs and POPs are porous networks containing thermally stable polymeric C=N bonds. The ability to capture CO_2 through R = N(δ^-)–C(δ^+)O$_2$ interactions have been recently studied using neutron scattering and X-ray diffraction techniques.[5] The realization of high CO_2 capture within a porous organic polymer depends on a number of factors such as chemical structure, porosity, thermal stability and isosteric heat of adsorption. Many other types of microporous and mesoporous amorphous sorbents have been studied as potential sorbents for CO_2 capture, such as nitrogen rich porous benzimidazole based polymers[1] (BILPs), which exhibited very good gas uptake and selectivity. Sulfur containing porous polymers showed a moderate CO_2 capture capacity at low pressures (1 bar), however they can adsorb exceptionally high amounts of CO_2 at high pressure.[2l] This article describes the synthesis and characterization of a conjugated porous organic polymer, IBTP, which contains both sulfur and nitrogen electron rich functional groups that retains a high amount of nitrogen content and binds CO_2. To the best of our knowledge, the use of an imine and benzothiazole functionalized porous polymer for CO_2 capture, or for H_2 and CH_4 storage, has not been reported thus far. The IBTP was prepared *via* a Schiff base condensation reaction between 1,3,5-tris-(4-formylphenyl)-benzene (**1**) and 2,6-diaminobenzo bisthiazole (**2**) in dimethylsulfoxide under reflux conditions for 72 hours (Scheme 1).

The IBTP porous polymer was isolated in 72% yield as a dark brown powder. It was thoroughly washed with anhydrous dioxane and *N*,*N*′-dimethylformamide and was totally insoluble in dimethylsulfoxide, dichloromethane, acetone, and tetrahydrofuran. This new material exhibited a CO_2 capture capacity of 7.8 wt% and a CH_4 adsorption capacity of 0.9 wt% at 273 K, 1 bar and an adsorption capacity of 0.78 wt% for H_2 at 77 K/1 bar. The chemical connectivity, components, crystallinity, porosity, and thermal stability of the IBTP porous polymer was determined by several analytical methods such as Fourier transform infrared spectroscopy (FT-IR) and solid-state ^{13}C CP-MAS NMR, elemental analysis, powder X-ray diffraction (PXRD), surface area measurements, and thermogravimetric analysis. The FT-IR spectrum of IBTP showed highly attenuated N–H and C=O stretching frequencies from the 1,3,5-tris-(4-formylphenyl)-benzene and 2,6-diaminobenzo bisthiazole at 3400 cm^{-1}, 3280 cm^{-1} and 1740 cm^{-1}. The formation of imine bonds between **1** and **2** (see ESI†) was confirmed by FT-IR which exhibited a new characteristic C=N stretching frequency at 1690 cm^{-1} (Fig. S1–S2, ESI†). Solid-state ^{13}C CP-MAS NMR measurements support the presence of benzothiazole and 1,3,5-tris-(4-formylphenyl)-benzene monomers in the framework. The IBTP polymer exhibited peaks at 169 and 156 ppm which

[a]*Department of Chemistry, University of Texas at El Paso, El Paso, TX 79968, USA. E-mail: echegoyen@utep.edu; Fax: +1-915-747-8807; Tel: +1-915-747-7573*

[b]*Department of Chemical Engineering, New Mexico State University, Las Cruces, NM 88003, USA*

† Electronic supplementary information (ESI) available: Experimental details, Fig. S1 and S9. See DOI: 10.1039/c3ra47587e

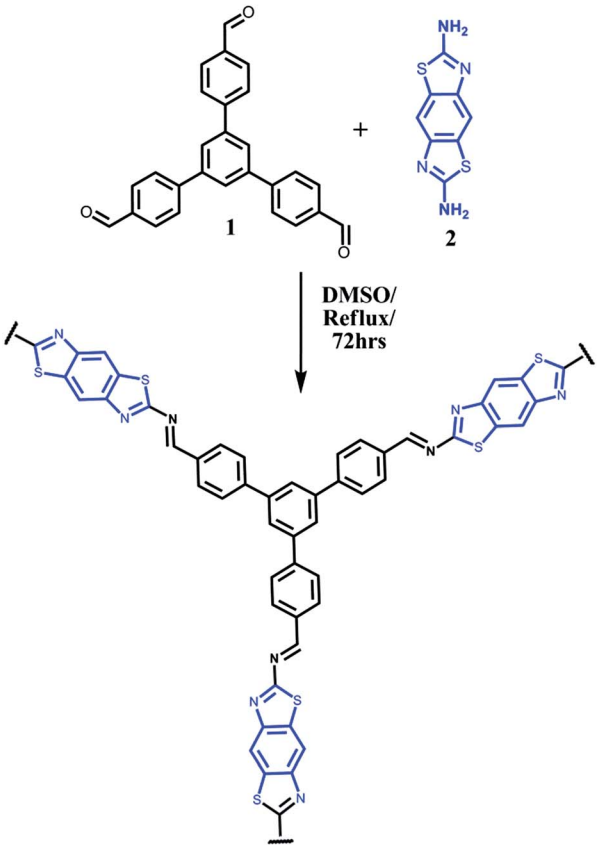

Scheme 1 Synthesis of IBTP from 1,3,5-tris-(4-formylphenyl)-benzene and 2,6-diaminobenzo bisthiazole.

correspond to the C═N (–C═N) carbons in the benzothiazole and imine units (Fig. S3, ESI†), respectively. In addition, the NMR spectrum also showed multiple peaks between 104 and 139 ppm which can be assigned to other aromatic carbon atoms from both building blocks. Powder X-ray diffraction (Cu Kα radiation) did not exhibit any diffraction peaks, as commonly observed for amorphous porous organic polymers (Fig. S4, ESI†).

N_2 gas adsorption–desorption measurements of degassed IBTP confirmed its microporosity at 77 K (Fig. 1). The apparent Brunauer–Emmett–Teller (BET) surface area was 328 $m^2\ g^{-1}$ and a surface area of 1705 $m^2\ g^{-1}$ was obtained by applying the Langmuir model. The steady N_2 uptake at low pressure (0–0.1 bar) and the gradual increase at higher pressures (0.1–1 bar) resulting a type I isotherm (Fig. 1a), which is typical for microporous frameworks that show permanent microporosity. This surface area is lower than others reported for imine linked polymers. Pore size distribution curves were analyzed by fitting the uptake of the N_2 isotherm using the nonlocal density functional theory (NLDFT) method, and were found to be around 15 Å (Fig. S5, ESI†) and the pore volume was calculated to be 0.81 $cm^3\ g^{-1}$. Hysteresis was observed with the desorption low lying above the adsorption, which could be due to the presence of micropores and diffusion of gas through micropores to mesopores that are also present in the framework and *vice versa*. To find the possible impact of the microporosity and nitrogen rich pore walls of IBTP, we measured CO_2, CH_4, N_2 and

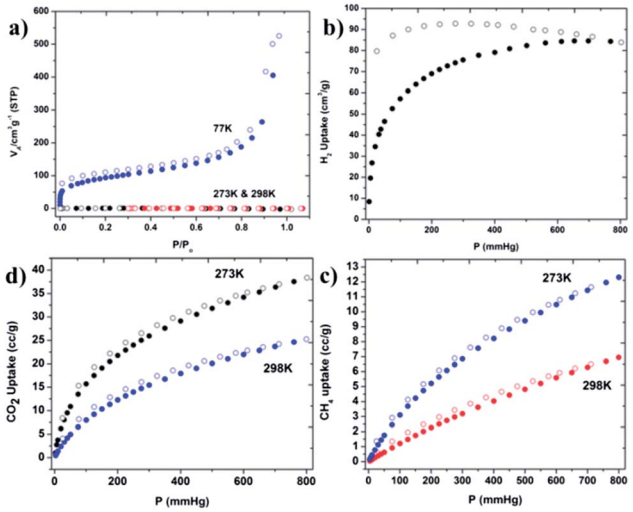

Fig. 1 (a) Nitrogen at 77 K; (b) hydrogen at 77 K; (c) CO_2 at 273 K and 298 K; (d) CH_4 at 273 K and 298 K adsorption (filled symbols) and desorption (empty symbols) isotherm curves.

H_2 adsorption capacities and selectivity and calculated their respective isosteric enthalpies (Q_{st}). All CO_2, CH_4 and N_2 isotherms were measured at 273 and 298 K from 0–1 bar (Fig. 1c and d). Both CO_2 and CH_4 isotherms are reversible and exhibit a steep rise at $P = 0$–1 bar, the CO_2 capture capacity of IBTP was 7.8 wt% at 273 K and 5 wt% at 298 K, respectively. The Q_{st} value for CO_2 was estimated from data collected under these conditions using the Van't Hoff equation. At zero coverage, the Q_{st} is 37.4 kJ mol^{-1} (Fig. S6, ESI†). The CO_2 uptake and Q_{st} are higher than the corresponding value for most COFs and for imine POPs and comparable to ZIFs containing nitrogen functionalized pores. The relatively high binding capacity of IBTP for CO_2 is likely due to favorable interactions between CO_2 molecules and the nitrogen rich imine and benzothiazole units in the framework. The reversible adsorption–desorption behavior indicates that CO_2 interactions with pore walls are weak enough to allow for IBTP regeneration without applying heat. Usually materials that have strong basic sites display high CO_2 affinities and require energy input in the form heat to regenerate their active sites as in the case of commercial amine solutions. In addition to CO_2 adsorption, we have evaluated the adsorption properties of N_2, H_2 and CH_4 on IBTP at low pressures and different temperatures due to their potential use in automobile applications. The H_2 uptake of IBTP shown in Fig. 1b, exhibited a reversible profile and pronounced hysteresis that we believe is due to the sulfur–hydrogen interactions. At 77 K, 1 bar, IBTP exhibited an uptake of 0.78 wt% which is comparable to other crystalline 2D COFs such as COF-10[2] (0.8 wt% at 77 K and 1 bar). Similarly, we measured CH_4 and N_2 storage properties on the IBTP polymer at both 273 K and 298 K, which revealed an uptake of 0.9 and 0.5 wt% for CH_4 at 273 K and 298 K/1 bar and almost zero for N_2 under similar conditions (Fig. 1d). Once again, both isotherms are reversible and exhibit a steep rise at low pressure for CH_4 and then reach maxima at 1 bar, 273 and 298 K, respectively. The Q_{st} for CH_4 was calculated using

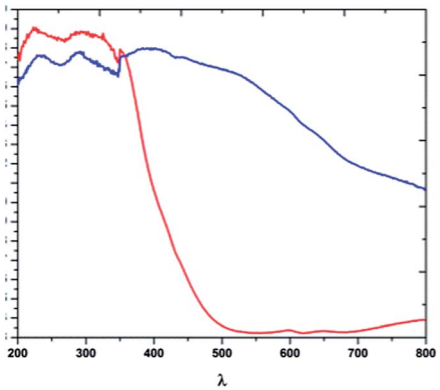

Fig. 2 Solid-state UV absorption spectra of IBTP (red) and 2,6-diaminobenzo bisthiazole (blue) obtained from powders using a praying mantis diffuse reflectance accessory.

adsorption data collected at 273 and 298 K. At zero coverage, the Q_{st} for CH_4 is 20.7 kJ mol^{-1} which is higher than for most COFs and POPs (Fig. S6, ESI†). A higher Q_{st} value for CO_2 compared to that of CH_4 is likely due to the $-N(\delta^-)-C(\delta^+)O_2$ interactions. Furthermore, the selectivity of IBTP towards CO_2 over N_2/CH_4 was investigated by collecting isotherms at 273 and 298 K (Fig. S6, ESI†). At 273 K and 1 bar, the CO_2 uptake is 7.8 wt% whereas that of CH_4 is only 0.9 wt%. On the basis of Langmuir model fits and Henry's constant values in the pressure range of 0 to 1 bar, the estimated adsorption selectivity for CO_2/N_2 is 51 and for CO_2/CH_4 it is 6.3 at 273 K/298 K/1 bar. Similar calculation methods have been reported for COPs, obtaining selectivities higher (63–109 at 273 K) than the IBTP.[2m] We also measured the absorption spectra of IBTP and diaminobenzo bisthiazole monomer to find the absorption ability of benzothiazole units in the UV-Vis region. The molecular organization of these benzothiazole chromophores in the porous polymer was evident from new absorption peaks at 595 and 640 nm, with the spectrum of monomer 2,6-diaminobenzo bisthiazole, while peaks at 230 and 290 nm (Fig. 2) were conserved. This proves the presence of benzothiazole chromophores in the IBTP polymer which is further evident from the color change of the polymer sample to dark brown whereas the monomers are white and yellow.

To measure the thermal stability, IBTP samples were subjected to thermogravimetric analysis under a flow of N_2 (Fig. S7, ESI†). The TGA trace is typical of the other reported POPs, retaining 80% of the mass at 450 °C. Visualization of these imine and benzothiazole based networks using scanning electron microscopy (SEM) showed randomly aggregated particles of IBTP powder, which did not provide any further insight into the porous nature of the framework (Fig. S8, ESI†).

Conclusions

In conclusion, we have synthesized a new nanoporous polymer, IBTP, containing nitrogen rich functional groups, an imine and benzothiazole groups, for the first time. The BET surface area of the IBTP was 328 m^2 g^{-1} and a CO_2 capture capacity of 7.8 wt% with very good selectivities of 51 and 6.3 compared to N_2 and CH_4 under similar conditions. This design strategy for extended π-conjugated molecules and the high chemical and thermal stabilities make it attractive for post synthetic modification for enhanced selective gas uptake. These aspects are currently under investigation.

Acknowledgements

This work was generously supported by NSF grant DMR-1205302 (PREM program), and the Robert A. Welch Foundation, grant # AH-0033.

References

1 (*a*) P. Kuhn, M. Antonietti and A. Thomas, *Angew. Chem., Int. Ed.*, 2008, **47**, 3450; (*b*) F. J. Uribe-Romo, J. R. Hunt, H. Furukawa, C. Klöck, M. O'Keeffe and O. M. Yaghi, *J. Am. Chem. Soc.*, 2009, **131**, 4570; (*c*) O. K. Farha, A. M. Spokoyny, B. G. Hauser, Y.-S. Bae, S. E. Brown, R. Q. Snurr, C. A. Mirkin and J. T. Hupp, *Chem. Mater.*, 2009, **21**, 3033; (*d*) P. Pandey, A. P. Katsoulidis, I. Eryazici, Y. Wu, M. G. Kanatzidis and S. T. Nguyen, *Chem. Mater.*, 2010, **22**, 4974; (*e*) P. Pandey, O. K. Farha, A. M. Spokoyny, C. A. Mirkin, M. G. Kanatzidis, J. T. Hupp and S. T. Nguyen, *J. Mater. Chem.*, 2011, **21**, 1700; (*f*) S. Wan, F. Gándara, A. Asano, H. Furukawa, A. Saeki, S. K. Dey, L. Liao, M. W. Ambrogio, Y. Y. Botros, X. F. Duan, S. Seki, J. F. Stoddart and O. M. Yaghi, *Chem. Mater.*, 2011, **23**, 4094; (*g*) S.-Y. Ding, J. Gao, Q. Wang, Y. Zhang, W.-G. Song, C.-Y. Su and W. Wang, *J. Am. Chem. Soc.*, 2011, **133**, 19816; (*h*) M. Hashem, C. G. Bezzu, B. M. Kariuki and N. B. McKeown, *Polym. Chem.*, 2011, **2**, 2190; (*i*) N. B. McKeown, *J. Mater. Chem.*, 2010, **20**, 10588; (*j*) M. G. Rabbani and H. M. El-Kaderi, *Chem. Mater.*, 2011, **23**, 1650; (*k*) M. G. Rabbani and H. M. El-Kaderi, *Chem. Mater.*, 2012, **24**, 1511; (*l*) M. G. Rabbani, T. E. Reich, R. M. Kassab, K. T. Jackson and H. M. El-Kaderi, *Chem. Commun.*, 2012, **48**, 1141; (*m*) T. E. Reich, S. Behera, K. T. Jackson, P. Jena and H. M. El-Kaderi, *J. Mater. Chem.*, 2012, **22**, 13524; (*n*) K. V. Rao, R. Haldar, C. Kulkarni, T. K. Maji and S. J. George, *Chem. Mater.*, 2012, **24**, 969; (*o*) Y. Zhu, H. Long and W. Zhang, *Chem. Mater.*, 2013, **25**, 1630; (*p*) Y. Jin, Y. Zhu and W. Zhang, *CrystEngComm*, 2013, **15**, 1484; (*q*) V. S. P. K. Neti, X. Wu, S. Deng and L. Echegoyen, *Polym. Chem.*, 2013, **4**, 4566.

2 (*a*) A. P. Côté, A. I. Benin, N. W. Ockwig, M. O'Keeffe, A. J. Matzger and O. M. Yaghi, *Science*, 2005, **310**, 1166; (*b*) R. W. Tilford, W. R. Gemmill, H.-C. zur Loye and J. J. Lavigne, *Chem. Mater.*, 2006, **18**, 5296; (*c*) E. L. Spitler and W. R. Dichtel, *Nat. Chem.*, 2010, **2**, 672; (*d*) X. Ding, J. Guo, X. Feng, Y. Honsho, J. Guo, S. Seki, P. Maitarad, A. Saeki, S. Nagase and D. Jiang, *Angew. Chem., Int. Ed.*, 2011, **50**, 1289; (*e*) M. Dogru, A. Sonnauer, A. Gavryushin, P. Knochel and T. Bein, *Chem. Commun.*, 2011, **47**, 1707; (*f*) J. W. Colson, A. R. Woll, A. Mukherjee, M. P. Levendorf, E. L. Spitler, V. B. Shields, M. G. Spencer, J. Park and

W. R. Dichtel, *Science*, 2011, **332**, 228; (*g*) X. Liu, Y. Xu, Z. Guo, A. Nagai and D. Jiang, *Chem. Commun.*, 2013, **49**, 3233; (*h*) M. G. Rabbani, A. K. Sekizkardes, Z. Kahveci, T. E. Reich, R. Ding and H. M. El-Kaderi, *Chem. – Eur. J.*, 2013, **19**, 3324; (*i*) X. Chen, M. Addicoat, S. Irle, A. Nagai and D. Jiang, *J. Am. Chem. Soc.*, 2013, **135**, 546; (*j*) V. S. P. K. Neti, X. Wu, S. Deng and L. Echegoyen, *CrystEngComm*, 2013, **15**, 6892; (*k*) V. S. P. K. Neti, X. Wu, M. Hosseini, R. Bernal, S. Deng and L. Echegoyen, *CrystEngComm*, 2013, **15**, 7157; (*l*) H. A. Patel, F. Karadas, J. Byun, J. Park, E. Deniz, A. Canlier, Y. Jung, M. Atilhan and C. T. Yavuz, *Adv. Funct. Mater.*, 2013, **23**, 2270; (*m*) H. A. Patel, S. H. Je, J. Park, D. P. Chen, Y. Jung, C. T. Yavuz and A. Coskun, *Nat. Commun.*, 2013, **4**, 1357.

3 (*a*) J. Sculley, D. Yuan and H.-C. Zhou, *Energy Environ. Sci.*, 2011, **4**, 2721; (*b*) K. Sumida, D. L. Rogow, J. A. Mason, T. M. McDonald, E. D. Bloch, Z. R. Herm, T. H. Bae and J. R. Long, *Chem. Rev.*, 2012, **112**, 724.

4 (*a*) B. Wang, H. Furukawa, M. O'Keeffe and O. M. Yaghi, *Nature*, 2008, **453**, 207; (*b*) R. Banerjee, A. Phan, B. Wang, C. Knobler, H. Furukawa, M. O'Keeffe and O. M. Yaghi, *Science*, 2008, **319**, 939; (*c*) A. Phan, C. J. Doonan, F. J. Uribe-Romo, C. B. Knobler, M. O'Keeffe and O. M. Yaghi, *Acc. Chem. Res.*, 2010, **43**, 58.

5 S. Yang, J. Sun, A. J. Ramirez-Cuesta, S. K. Callear, W. I. F. David, D. P. Anderson, R. Newby, A. J. Blake, J. E. Parker, C. C. Tang and M. Schröder, *Nat. Chem.*, 2012, **4**, 887.

